

# Optical properties of $\text{PbI}_2$ films: Quantum confinement and residual stress effect

Vikash Gulia and A. G. Vedeshwar\*

*Thin Film Laboratory, Department of Physics and Astrophysics, University of Delhi, Delhi-110007, India*

(Received 15 July 2006; revised manuscript received 11 December 2006; published 9 January 2007)

The optical properties of vacuum-evaporated, stoichiometric, well-characterized  $\text{PbI}_2$  films exhibit quantum-dot-like behavior and strain dependence. The shifts in optical peaks obey a linear behavior with the strain determined by x-ray diffraction. The energy shift due to residual stress can be separated from the measured data to obtain the contribution of only the confinement effect. The optical peak at around 3 eV shows a systematic blueshift with decrease of the grain size  $D$ . The observed linear dependence of the 3 eV peak on  $1/D^2$  indicates a typical quantum-dot-like behavior and yields the corresponding bulk value of the transition as 2.98 eV and the reduced effective mass of the involved electron-hole pair as  $0.15m_e$ . This study shows that an appropriate choice of the concerned bulk optical transitions (not merely the minimum energy gap) is necessary for correctly interpreting the grain-size-induced blueshift of optical peaks for anisotropic and complex band structure materials like  $\text{PbI}_2$ . The pressure coefficients of a few optical transitions are determined from the strain dependence.

DOI: [10.1103/PhysRevB.75.045409](https://doi.org/10.1103/PhysRevB.75.045409)

PACS number(s): 81.07-b, 61.46.Df, 78.67.-n

## I. INTRODUCTION

The growth and characterization of nanosize semiconductors are becoming increasingly important in recent years. It is well established that the electronic properties of low-dimensional materials exhibit a striking quantum size effect.<sup>1</sup> The zero-dimensional structures [three-dimensional (3D) spatial confinement] known as quantum dots (QDs) can be synthesized in the form of very thin discontinuous films, colloidal suspensions, particles embedded in different media, self-assembled structures, and so on.<sup>2</sup> All materials having natural layered structures (like metal dihalides, chalcogenides, etc.) are expected to facilitate the growth of zero-dimensional quantum-confined nanostructures due to their anisotropy along the directions parallel and perpendicular to the  $c$  axis and the stacking of weakly bound halide-metal-halide layers along the  $c$  axis. Lead iodide ( $\text{PbI}_2$ ) is one such material investigated to some extent in this direction. For example, ultrathin films,<sup>3-5</sup> and colloidal nanoclusters<sup>6-8</sup> of  $\text{PbI}_2$  have been investigated for quantum confinement effects. Ultrathin microcrystallites of  $\text{PbI}_2$  embedded in polymer<sup>9</sup> have also been studied. Most of these studies demonstrate the quantum confinement effect mainly by optical absorption measurements. However, the interpretations of the absorption spectra entirely differ from one reference to another. Bulk  $\text{PbI}_2$  itself shows quite complex optical spectra indicating the complex nature of its band structure. It would be very reasonable to take the bulk optical spectra as reference for interpreting the quantum confinement effects. Also, the measured optical transition energies may have combined contributions due to various effects like temperature, residual stress (very common in films), quantum confinement, and so on. Therefore, in this paper we have studied the effects of quantum confinement and residual stress on the optical properties of  $\text{PbI}_2$  films using both our experimental data and literature data.

## II. EXPERIMENT

$\text{PbI}_2$  films were grown on glass substrates ( $2 \times 6$  cm) at both room and low temperatures ( $\sim 80$  K) by thermal evapo-

ration using a molybdenum boat. The starting material [high-purity (99.999%) stoichiometric powder] was palletized for evaporation. All the films were grown at a base vacuum of  $10^{-6}$  Torr. The deposition rate was optimized at 1–2 nm/s to grow uniform good-quality films. The film thickness and deposition rate were monitored during the film growth by a quartz crystal thickness monitor (HINDHIVAC, model 101). The film thickness was subsequently controlled by a mechanical stylus method within an error of  $\pm 1$  nm using a DEKTEK IIA surface profiler. The film stoichiometric analysis was done using x-ray photoelectron spectroscopy (XPS) (Perkin Elmer mode1257 ESCA/Auger) and energy dispersive x-ray analysis (EDAX) (JEOL-840). The structural analyses of the films were carried out by x-ray diffraction (XRD) (PHILIPS X-Pert PW1830 diffractometer). The morphology (and also the structure in diffraction mode) of the films was studied by transmission electron microscopy (TEM) (JEOL-JEM 2000EX microscope). For TEM studies, films were grown on polymer-coated copper grids placed on the substrates. The optical absorption measurements were carried out using a uv-visible fiber-optics-based spectrophotometer (Ocean Optics HR-4000). Small pieces ( $1 \times 1$  cm<sup>2</sup>) of the same film were used for various analyses. All these measurements and analyses can be considered as very accurate because of the modern computer interfacing and analysis software. All the measurements in the present work were carried out at room temperature ( $\sim 300$  K).

## III. RESULTS AND DISCUSSIONS

We have systematically analyzed a large number of samples grown by varying one growth parameter at a time (like film thickness, growth temperature, deposition rate, vacuum-annealing temperature and duration, etc.) while keeping all the other parameters fixed. All the characterizations were done on the same sample. Both XPS and EDAX confirm the films as stoichiometric. No noticeable change in stoichiometry was observed in any sample more than the experimental error (0.3% maximum). We mainly try to cor-

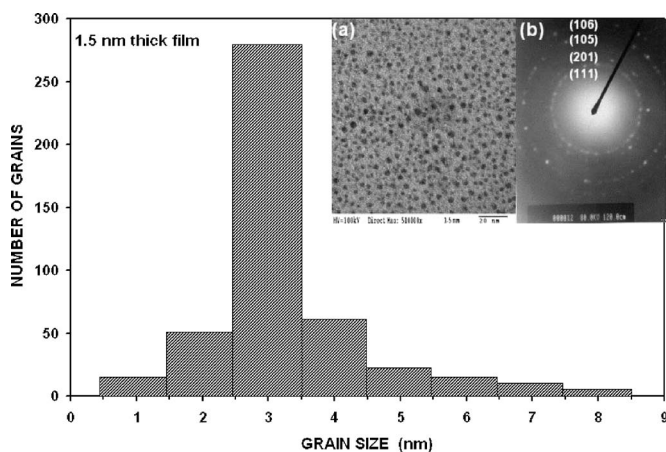


FIG. 1. Grain size distribution determined from TEM of 1.5-nm-thick film shown in inset (a). Inset (b) is its diffraction mode.

relate the grain size and residual strain with the optical properties. However, for reasons of clarity and brevity, we do not intend to show the parametric dependences of grain size and residual stress. Therefore, we have gathered the data on the optical spectra of the samples for which grain size and residual stress were determined from all these experiments.

The structure and grain sizes were determined for ultrathin films using TEM. A representative TEM micrograph and the corresponding electron diffraction pattern are shown in the insets of Fig. 1 for 1.5-nm-thick film. The  $d$  spacings (with the Miller indices indicated on the micrograph) calculated from the radius of the rings [inset (b)] match quite well with ASTM card no. 07-0235 for the  $2H$  polytype of  $PbI_2$ . Since the diffraction in TEM is only by a few discontinuous grains, it may not indicate any specific overall growth orientation. It is only used to characterize the films by comparison of  $d_{hkl}$  with those from the bulk powder diffraction data card mentioned above. The good agreement between the two also confirms the stoichiometry. Further, the particle or grain size is determined quite accurately especially for (1–10)-nm-thick films from the size distribution profile of TEM images similar to that shown in Fig. 1. The size distribution was found to be more homogeneous or monodisperse (unimodal) for thinner films as can be seen from the inset (a) of Fig. 1. However, TEM was used only for film thickness  $\leq 20$  nm. For thicker films, we have observed the melting of smaller grains followed by the formation of merged bigger grains during the focusing, probably induced by the electron beam at 100 kV. This is probably due to the low melting point of  $PbI_2$  (400 °C). The peak value of the grain size distribution (unimodal) was taken as the mean or average grain size for our further analyses. Grain size grows linearly with film thickness. Figure 2 shows few representative XRD patterns. It clearly shows the growth of the preferred (00 $l$ ) orientation (parallel to the substrate plane, or  $c$  axis perpendicular to the substrate plane) indicated by the presence of only (00 $l$ ) peaks.  $PbI_2$  seems to have a very strong affinity for growth in this preferred orientation. This is further evidenced by the fact that no other peaks are observed in any sample without exception, irrespective of the growth and process parameters. The full width at half maximum (FWHM) of the most in-

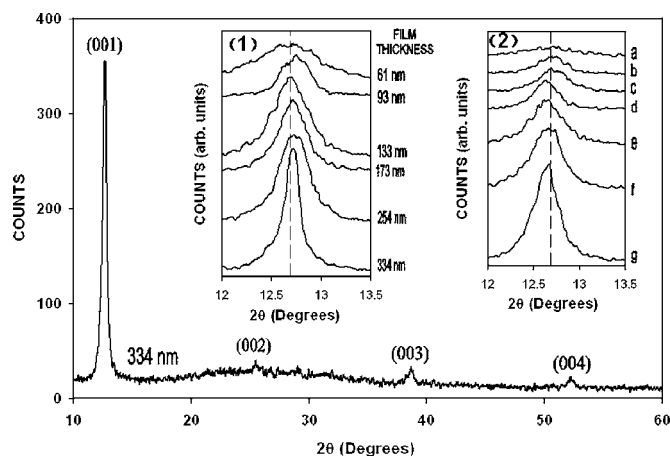


FIG. 2. Typical XRD of  $PbI_2$  films depicting (001) preferred orientation of growth. Insets show both types of residual stress developed in various kinds of samples. Inset (1) shows the deviation of the (001) peak from the ASTM value (represented by the broken vertical line) for various film thicknesses as identified. Inset (2) shows similar behavior for samples *a*, 254-nm-thick film grown at liquid nitrogen temperature (LNT); *b*, 173-nm-thick film grown at LNT and vacuum annealed at 200 °C for 2 h; *c*, 254-nm-thick film grown at room temperature (RT); *d*, 334-nm-thick film grown at LNT; *e*, 93-nm-thick film grown at RT and annealed at 300 °C for 3 h; *f*, 93-nm-thick film grown at LNT and annealed at 200 °C for 3 h; and *g*, 173-nm-thick film grown at RT and annealed at 200 °C for 2 h.

tense peak in the XRD pattern is routinely used to determine the average particle (or grain) size using the Scherrer formula.<sup>2,10</sup> We have determined the average grain sizes for films thicker than 10 nm using XRD. The variation of grain size in various samples is also evident in the insets of Fig. 2 by the variation in the FWHM. The average grain size determined by XRD agrees quite well with the peak value of the grain size distribution determined by TEM as observed on the samples for which both the measurements were possible. Similar agreement has been observed for  $HgTe$ .<sup>10</sup>

A few optical absorption spectra for various thicknesses are displayed in Fig. 3. Peaks in the spectra are alphabetically labeled, in increasing order of energy, as the expected optical transitions for bulk (or thick film)  $PbI_2$ . We have summarized the optical properties of  $PbI_2$  including results from earlier works and available band structure calculations in Table I for reference and convenience of further discussions. The labeling of the peaks is in accordance with the table. Only peak *B* appears for film thickness  $\leq 20$  nm. The blueshifting of peak *B* with decreasing film thickness is clearly visible in the figure. Peak *C* starts appearing for films  $\geq 25$  nm thick followed by the appearance of peak *A* for films  $\geq 30$  nm thick. However, the fourth peak *D* expected around 3.6 eV in bulk seems to appear as a broad hump in almost all the samples. Since the spectra become noisy and the determination of peak *D* becomes difficult, we have not analyzed it further. The transition at 3 eV corresponds to the  $M_1$  three-dimensional saddle point and can only be explained by taking into account the interaction between different layers.<sup>11</sup> In colloidal nanoparticles, the peak *A* at around 2.5 eV is completely absent and blueshifted peaks *B* and *C*

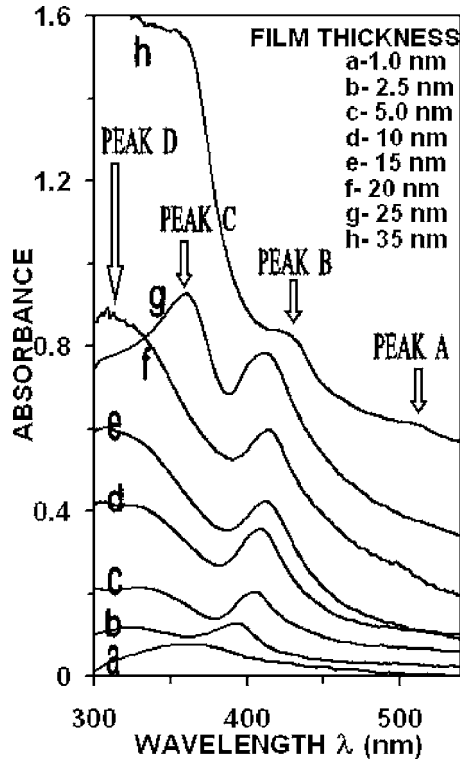


FIG. 3. Thickness-dependent optical absorption of ultrathin PbI<sub>2</sub> films grown at room temperature. The film thickness and various peaks are identified in the figure. Spectra are vertically shifted for clarity.

appear along with one or two higher-energy structures.<sup>6–8</sup> In the light of the above discussion, it seems the appearance of peak A requires a critical lateral dimension of the grain, which we determine to be about 15 nm in the present study. This fact is further justified by Ref. 9 in which the lateral size of platelet-shaped crystallites observed by TEM is in the range 2–80 nm (exact grain size not mentioned for the measured spectra) and all the peaks are observed, in contrast with colloidal particles of size less than 3–5 nm. These observations are quite consistent with the band structure calculations and their assignment of transitions explained above. Therefore, the evolution of absorption spectra with film thickness (or grain size) observed here can be viewed as moving from the quantum confinement regime to bulklike behavior.

A careful quantitative analysis of TEM and XRD results shows small strain in the *d* spacings due to the residual stress developed during the vapor condensation. The strain is calculated for all the samples using the only intense peak (001) in the XRD by the relation

$$\frac{\Delta d}{d} = \frac{d_{001}(\text{observed}) - d_{001}(\text{ASTM})}{d_{001}(\text{observed})} \quad (1)$$

where  $d_{001}$  is the lattice spacing of the (001) planes. The observed strain is very nominal for films up to 10 nm thick as determined by TEM, probably because of the isolated and small grains in the discontinuous film. Thicker films show increasing strain with film thickness. Polycrystalline films usually have intragranular and intergranular (at grain boundaries) residual stresses. XRD determines the intragranular

TABLE I. Summary of the optical properties of PbI<sub>2</sub> (2*H* polytype) in the range 2.5–4.5 eV.

Theory (Refs. 11 and 12)		Optical transitions					
		Experimental (absorption) peaks (eV)					
Peak (eV)	Assignment	Bulk and films Refs. 13 and 14	Thick films Present work (stress-free values)	QD (colloidal)	QD (colloidal)	QD (colloidal)	QD (ultra thin film)
				Ref. 6	Ref. 7	Ref. 8	Present work
				$D_{av} \approx 2.3$ nm (by TEM)	$D_{av} \approx 2.1$ nm (by TEM)	$D \approx 1.3$ nm (calculated)	$D \approx 2.2$ nm (by TEM)
(A) 2.5	$A_4^+ \rightarrow A_4^-$ ( $M_0$ type) <sup>a</sup> Excitonic, band edge	2.51 <sup>b</sup>	2.5				
(B) 3.0	$\Gamma_4^+ \rightarrow \Gamma_4^-$ ( $M_1$ type) <sup>a</sup> 3D saddle point	3.08 <sup>b</sup>	2.98	3.42	3.46	3.38, 3.45	3.44
(C) 3.3	$A_4^+ \rightarrow (A_5^-, A_6^-)$ ( $M_0$ type) Excitonic <sup>a</sup>	3.32 <sup>b</sup>	3.33				
(D) 3.6	$\Gamma_4^+ \rightarrow \Gamma_5^-$ ( $M_1$ type) <sup>a</sup> 3D saddle point	3.6 <sup>c</sup>	3.58	3.95		3.86	
(E) 3.9	$A_4^+ \rightarrow A_4^-$ ( $M_0$ type) <sup>d</sup> Excitonic	3.9 <sup>c</sup>			4.31	4.1, 4.25	
(F) 4.3	$\Gamma_4^+ \rightarrow \Gamma_6^-$ ( $M_1$ type) <sup>d</sup> 3D saddle point	4.3 <sup>c</sup>		4.8		4.48	
(G) 4.5	$\Gamma_4^+ \rightarrow (\Gamma_5^-, \Gamma_6^-)$ ( $M_1$ type) <sup>d</sup> 3D saddle point	4.5 <sup>c</sup>				4.75	

<sup>a</sup>References 11 and 12.

<sup>b</sup>References 13 and 14.

<sup>c</sup>Reference 14.

<sup>d</sup>Reference 12.

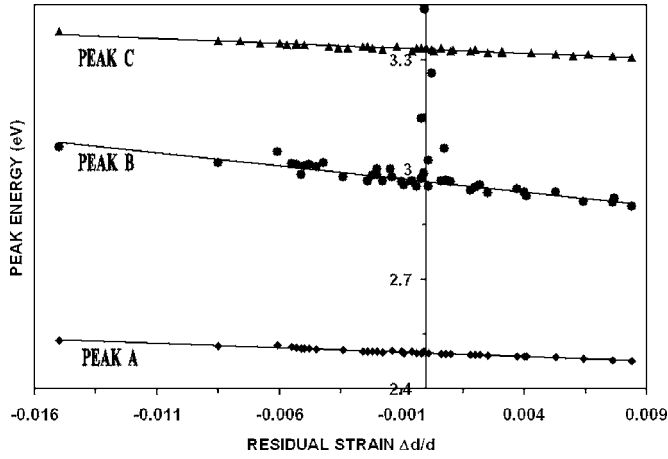


FIG. 4. Linear correlation between the residual strain  $\Delta d/d$  and the three peaks A, B, C labeled in the optical absorption spectra for  $\text{PbI}_2$  films. The straight line represents a least-squares fit for the data points connected by it.

stress along the film thickness while interferometric methods determine the intergranular stress along the film thickness.<sup>15</sup> The film will be stable as long as these two stresses are in equilibrium or compensate each other. Since our films were very stable (without any crack), these two stresses must be of opposite types, compensating each other. This is quite reasonable because similar behavior and magnitude of intergranular residual stress measured by interferometry is reported<sup>16</sup> for some vacuum-evaporated halide films including  $\text{PbCl}_2$ . Stress is expected to affect the band structure and hence the optical transitions too. Therefore, we have plotted three peaks as a function of strain in Fig. 4 to look for any correlation. A linear relation can be seen in the figure for all three peaks. Only in case of peak B do some points (having negligible strain) deviate drastically from this trend. The measured energy of peak B has contributions from both size quantization and residual stress. The stress contribution can be subtracted using the slope  $(-8.35 \text{ eV})/(\Delta d/d)$  for peak B for the strain correction.

In order to analyze the quantum confinement effect, we plot in Fig. 5 the position of peak B as a function of the grain size  $D$  along with its  $1/D^2$  dependence as shown in the inset. All the quantities are identified in the figure. We have shown only strain-corrected (omitting the measured ones) values of peak B for the purpose of clarity and to separate the residual stress effect. We have also included two relevant data points from earlier reports<sup>6,7</sup> for which grain size was determined by TEM, for the purpose of analysis and comparison. Theoretically, the optical transition due to quantum confinement as a function of crystallite or grain size  $D$  including the Coulomb interaction term is given by<sup>1,2</sup>

$$E_n(D) = E_n(b) + \frac{\hbar^2 \pi^2}{2\mu D^2} - \frac{1.8e^2}{\epsilon D} \quad (2)$$

where  $E_n(D)$  is the observed grain-size-dependent optical transition and  $E_n(b)$  is its corresponding bulk value,  $\mu$  is the reduced effective mass of the electron-hole pair, and  $\epsilon$  is the dielectric constant (20.8 for  $\text{PbI}_2$  films<sup>14</sup>) of the material.

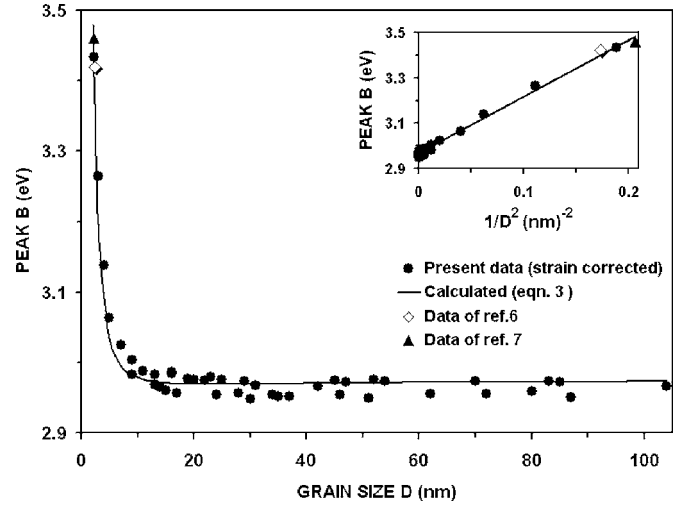


FIG. 5. Grain size dependence of peak B for all the samples of  $\text{PbI}_2$  films studied in the present work. Various symbols are identified in the figure and explained in the text. The inset depicts the  $1/D^2$  dependence of peak B, revealing the quantum confinement effect.

However, the contribution of the Coulomb term in the above equations becomes almost negligible for materials having  $\epsilon$  as large as  $\text{PbI}_2$ . For an isotropic semiconductor of fairly simple band structure having a direct band gap, Eq. (2) predicts enhancement in the bulk band gap [simply taking  $E_n(b) = E_g$ ] proportionate to the decreasing grain size. However, for anisotropic materials of complex band structure like  $\text{PbI}_2$ , the features of the band structure observed in the optical spectra for a bulk sample would blueshift with decreasing grain size in accordance with Eq. (2). We have determined  $E_B(b) = 2.98 \text{ eV}$  (very close to the bulk transition at 3 eV) and  $\mu = 0.15$  (from the slope) for peak B by its  $1/D^2$  dependence (neglecting the Coulomb term) shown in the inset of Fig. 5. Using these values, the continuous curve in Fig. 5 shows Eq. (2) illustrating the blueshift of peak B with decreasing grain size. Agreement between the observed (including the data from an earlier report) and calculated values is quite good. A similar analysis could have been carried out for other features like peaks A or C provided the grain size dependence is available in the confinement regime, which is not possible from the present study. However, we expect a more or less similar shift for all observable optical features from those of the bulk.

We also try to understand the few relevant data from earlier reports which are in good agreement with the present analysis as shown in Fig. 4. Both earlier attempts<sup>6,7</sup> on colloidal  $\text{PbI}_2$  nanoclusters analyze the observed peaks [one common (peak B) and two different (peaks D and E); see Table I] in their optical spectra using a relation [similar to Eq. (2)] containing two separate terms for quantization in the  $xy$  plane and along the  $z$  direction. They attributed the appearance of three peaks to three different cluster sizes. However, for InAs QDs it is shown that (Ref. 2, pp. 89–91) (a) the size distribution leads to inhomogeneous broadening of the absorption peaks and (b) the well-resolvable higher-energy peaks correspond to higher excited states. This fact is

TABLE II. Summary of the pressure effect on the optical transitions of PbI<sub>2</sub> (2H polytype).

Peak energy (eV)	Pressure coefficient ( $\partial E/\partial P$ ) <sub>T</sub> (meV/GPa)				Stress-free value from present work (eV)
	Ref. 13	Ref. 19	Ref. 20	Present work	
(A) 2.5	-172	-181	-91 to -175	-53	2.5
(B) 3.0	-56			-152	2.98
(C) 3.3	-13			-48	3.33
(D) 3.6	-87			-12	3.58

fairly well established for various semiconductors QDs either colloidal or grown in matrices, as evident from the literature.<sup>17</sup> In another similar study<sup>8</sup> on PbI<sub>2</sub> such peaks are interpreted as due to transitions between levels of different quantum numbers, and the grain size is calculated by fitting the observed transitions to a theoretical formula for a confining cylindrical potential. In doing so, the authors obtain different transitions for different quantum numbers, keeping the grain size almost the same. Also, all of them<sup>6–8</sup> determine  $\Delta E [= E_n(D) - E_n(b)]$  of various peaks from a fixed reference called the band gap  $E_g = 2.57$  eV, which therefore gives very large values of  $\Delta E$  for the peaks at higher energies. To account for such a large shift, a separate quantization term along the  $z$  direction was invoked, which gives a larger magnitude of  $\Delta E$  for a single layer of 0.7 nm. Therefore, this kind of interpretation of the results does not seem to be appropriate at least for PbI<sub>2</sub> for the reasons explained above. Using the present approach, a careful analysis reveals a very consistent and definite fact in all three earlier reports.<sup>6–8</sup> For example, the three peaks at 3.42, 3.95, and 4.8 eV (Ref. 6) give almost the same  $\Delta E = 0.42, 0.35,$  and  $0.5$  eV when measured from their corresponding bulk values 3, 3.6, and 4.3 eV.<sup>12</sup> This means that  $\Delta E$  is in accordance with  $D$  and its small variation for different transitions could be reflecting a slightly different reduced effective mass for different bands. In order to interpret correctly the results of the blueshifted optical peaks of the nanoparticles, it is necessary to identify the appropriate corresponding bulk transitions. Similarly, the results of the other two reports can also be interpreted very consistently. This is the reason why their data corresponding to peak  $B$  included in Fig. 5 agree so nicely with the present interpretation, taking their average grain size from TEM. The agreement is also not surprising from the point of view of effective masses. Taking the values used in Ref. 7 (in units of the free electron mass),  $m_{e\perp} = 0.55,$   $m_{e\parallel} = 0.38,$   $m_{h\perp} = 0.35,$  and  $m_{h\parallel} = 1.67,$  we can get  $m_e = 0.22$  and  $m_h = 0.29,$  combining the parallel and perpendicular components. These give the reduced effective mass of the electron-hole pair  $\mu = 0.125$  which is quite close to the one determined from the present study as mentioned above. However, it should be noted that there are quite diverse values of electron and hole effective masses for PbI<sub>2</sub> in the literature.

The reasonably good linear correlation between the peak energies and strain shown in Fig. 4 indicates unambiguously the cause of the peak shift as due to the residual stress. We can estimate the pressure coefficient  $(\Delta E/\Delta P)_T$  of the peaks

from the slopes of their linear behavior, provided the elastic constant of PbI<sub>2</sub> is known. Unfortunately and surprisingly, the elastic constant for PbI<sub>2</sub> is not available in the literature. Still, we can use the value<sup>18</sup> (appropriate along the  $c$  axis)  $C_{11} = 49.1$  GPa of an isostructural material CdI<sub>2</sub> for the purpose of estimation. Table II compares the calculated pressure coefficients with those found in the literature obtained by applying external pressure on bulk or films<sup>13,19</sup> or on microcrystals embedded in polymer.<sup>20</sup> For strain along the  $c$  axis, the pressure coefficients determined in this study reveal a different trend from previous reports.<sup>13,19</sup> In particular, the coefficients we deduce [ $-53$  meV/GPa (peak  $A$ ) and  $-152$  meV/GPa (peak  $B$ )] are almost reversed ( $-172$  and  $-56$  meV/GPa) from the corresponding values presented in Ref. 13. Our observed greater sensitivity of peak  $B$  to pressure is consistent with this transition being responsive to interactions between layers stacked perpendicular to the  $c$  axis. Since peak  $A$  is ascribed to the cationic layer, it would be more susceptible if the pressure were directed parallel to the layers.

A similar reversal for the other two peaks  $C$  and  $D$  in comparison with Ref. 13 is evident from Table II. The stress-free values of all the peaks determined by extrapolation from Fig. 4 are shown in the last column of Table II; they are very close to the theoretical and most accepted ones.

#### IV. CONCLUSIONS

PbI<sub>2</sub> films grown by vacuum evaporation show shifts of the optical peaks due to quantum confinement if they are very thin (1–20 nm) and due to residual stress for larger thickness (30–400 nm). The optical peaks red- or blueshift depending on the type of residual stress and this contribution can be separated from the measured values due to their linear relationship. The present study clearly suggests that an appropriate choice of the optical transition of the bulk is necessary for correctly determining and interpreting the quantum confinement effect in anisotropic and complex materials. This approach can consistently explain the results of similar earlier reports and demonstrates the adequacy and applicability of the simple theory of quantum confinement in explaining the measurements. Thus, optical transitions in PbI<sub>2</sub> are sensitive to quantum confinement and residual stress wherein both can lead to comparable energy shifts. For proper interpretation of results, it is important to identify the correspond-

ing transitions in bulk and isolate the effects of confinement from those of residual stress.

#### ACKNOWLEDGMENTS

The financial support of UGC, India in the form of Major Research Project No. F-10-24/2003(SR) for this work is

gratefully acknowledged. One of the authors (V.G.) would like to thank the University Grants Commission for partial financial support. We would also like to thank P. C. Padmakshan and Rohtash, Department of Geology, University of Delhi, for carrying out x-ray diffraction measurements and N. C. Mehra, USIC for TEM measurements.

---

\*Electronic address: agni@physics.du.ac.in

<sup>1</sup>A. D. Yoffe, *Adv. Phys.* **51**, 799 (2002), and references therein.

<sup>2</sup>*Nanoparticles: From Theory to Application*, edited by Gunter Schmid (Wiley-VCH, Weinheim, 2004).

<sup>3</sup>V. V. Mussil, V. K. Miloslavskily, A. I. Ribalka, and N. V. Tien, *Solid State Commun.* **17**, 1025 (1975).

<sup>4</sup>T. Goto and J. Maeda, *J. Phys. Soc. Jpn.* **56**, 3710 (1987).

<sup>5</sup>E. P. Pokatilov, S. I. Beril, V. M. Fomin, V. G. Litovchenko, D. V. Korbutyak, E. G. Lashkevich, and E. V. Mikhailovskya, *Phys. Status Solidi B* **145**, 535 (1988).

<sup>6</sup>C. J. Sandroff, D. M. Hwang, and W. M. Chung, *Phys. Rev. B* **33**, 5953 (1986).

<sup>7</sup>O. I. Micic, L. Zongguan, G. Mills, J. C. Sullivan, and D. Meisel, *J. Phys. Chem.* **91**, 6221 (1987).

<sup>8</sup>K. Mallik and T. S. Dhami, *Phys. Rev. B* **58**, 13055 (1998).

<sup>9</sup>S. Saito and T. Goto, *Phys. Rev. B* **52**, 5929 (1995).

<sup>10</sup>A. L. Rogach, S. V. Kershaw, M. Burt, M. Harrison, A. Kor-

nowski, A. Eychmuller, and H. Weller, *Adv. Mater. (Weinheim, Ger.) (Weinheim, Ger.)* **11**, 552 (1999).

<sup>11</sup>E. Doni, G. Grosso, and G. Spavieri, *Solid State Commun.* **11**, 493 (1972).

<sup>12</sup>I. Ch. Schluter and M. Schluter, *Phys. Rev. B* **9**, 1652 (1974).

<sup>13</sup>J. B. Anthony and A. D. Brothers, *Phys. Rev. B* **7**, 1539 (1973).

<sup>14</sup>I. Imai, *J. Phys. Chem. Solids* **22**, 81 (1961).

<sup>15</sup>A. E. Ennos, *Appl. Opt.* **5**, 51 (1966).

<sup>16</sup>D. S. Campbell, in *Handbook of Thin Film Technology*, edited by L. I. Maissel and R. Glang (McGraw-Hill, New York, 1970), pp. 12–22.

<sup>17</sup>U. Woggon, *Optical Properties of Semiconductor Quantum Dots* (Springer-Verlag, Berlin, 1997).

<sup>18</sup>*Semiconductors—Basic Data*, edited by O. Madelung, 2nd ed. (Springer-Verlag, Berlin, 1996), p. 188.

<sup>19</sup>M. J. Powell, *Philos. Mag. B* **38**, 71 (1978).

<sup>20</sup>S. Saito and T. Goto, *Solid State Commun.* **84**, 1043 (1992).